Int. J. Heat Mass Transfer. Vol. 14, pp. 1275–1284. Pergamon Press 1971. Printed in Great Britain

EFFICIENCY CHARACTERISTICS OF HEMI-ELLIPSOIDAL AND HEMISPHERICAL COLLECTORS OF THERMAL RADIATION

R. P. HEINISCH

Honeywell, Inc., Systems and Research Division, St. Paul, Minnesota, U.S.A.

and

E. M. SPARROW

Department of Mechanical Engineering, University of Minnesota, Minneapolis, Minnesota, U.S.A.

(*Received* 31 *August* 1970 *and in revised form* 5 *November* 1970)

Abstract—Collection efficiencies are determined for integrating hemi-ellipsoids and integrating hemispheres used in connection with radiation surface property measurements. The Monte Carlo method is employed to simulate the trajectories of photon bundles which leave a source of radiation and are collected and focused onto (or adjacent to) a receiver. The radiation source may be a test surface whose reflectance or emittance is to be determined, while the receiver may be a radiation detector. Results are obtained for a wide range of source and receiver sizes and positions. The results show that in the case of the hemi-ellipsoid, the attainment of good collection efficiency requires that the radius of the receiver be at least twice that of the source. The hemisphere is, in general, a less efficient collector than the hemi-ellipsoid. When the source and receiver are only slightly displaced from the center of the base plane circle of the hemisphere, then the two collectors are comparably efficient.

NOMENCLATURE

a, semi-major radius;
b, semi-minor radius;
e_i, incident energy flux per unit time and area;
F, displacement distance of source or receiver, Fig. 2;
f, focal distance;
R, radius of hemisphere;
r, radial coordinate of departure point;
r_r, radius of receiver;
r_s, radius of source;
x, y, z, coordinates;
$\hat{x}, \hat{y}, \hat{z}$, dimensionless coordinates, equation (5);
η, collection efficiency, equation (10);
θ, ϕ, departure angles, Fig. 2;
ρ_{bd}, bidirectional reflectance;
ψ, angular coordinate of departure point.

Subscripts

1, point of departure;
2, point of intersection with reflecting surface;
3, point of impingement on base plane.

INTRODUCTION

THIS paper is concerned with the characteristics of integrating hemi-ellipsoidal and hemispherical collectors of thermal radiation. Such instruments may be employed to collect the radiant energy reflected or emitted by a test surface and to focus the thus-collected energy onto a receiver, thereby facilitating the determination of the reflectance or the emittance. Both the test specimen and the receiver are situated in the base plane of the collector, while the curved

hemi-ellipsoidal (or hemispherical) surface is highly reflective and specular.

An ideal integrating collector is one in which all of the radiant energy leaving the test surface is focused onto the receiver. The utility of real collectors may be characterized by an efficiency which compares the radiant energy incident on the receiver to that leaving the test surface. The objective of this investigation is to determine collection efficiencies for hemi-ellipsoidal and hemispherical collectors as a function of the size and location of the test surface and of the receiver. The method of analysis makes use of probability sampling (i.e. Monte Carlo).

The use of an integrating hemispherical collector as a component of a reflectometer has been described in some detail in standard textbooks and survey articles [1–3] and in research reports on radiation property determinations (e.g. [4, 5]). In contrast to the integrating hemisphere, the hemi-ellipsoid has heretofore been used only sparsely in practice. Very recently, practical fabrication techniques for integrating hemi-ellipsoids have been developed [6]. As a consequence, these instruments are now available as practical tools for the determination of radiation properties.

The focusing properties of hemi-ellipsoidal and hemispherical collectors have been previously considered by Brandenberg [7]. He obtained geometrical relations for tracing the paths of rays from the test surface to the receiver. However, no provision was made for taking account of the spatial and directional distributions of the radiation leaving the test surface, and there are no results given for the collection efficiency.

Inasmuch as the hemisphere is a hemi-ellipsoid having equal major and minor axes, the former can be treated as a special case of the latter. Therefore, the analytical development is directed primarily toward the hemi-ellipsoid, with modifications incorporated for the hemisphere wherever relevant. Numerical results are presented for the collection efficiencies of both configurations.

ANALYSIS

The description of the analysis is facilitated by reference to Figs. 1 and 2. The first of these is a pictorial view of an integrating hemi-ellipsoid, the base of which lies in the x–y plane. The test surface, hereafter referred to as the source of radiant energy, is a circular region centered at one of the foci of the base plane ellipse. The receiver, also a circular region, is centered at the other focus of the base ellipse. The figure depicts the path of a typical photon bundle which leaves the source, reflects specularly on the surface of the ellipsoid, and impinges on the receiver. From the standpoint of geometrical optics, the photon bundle may be treated as a ray.

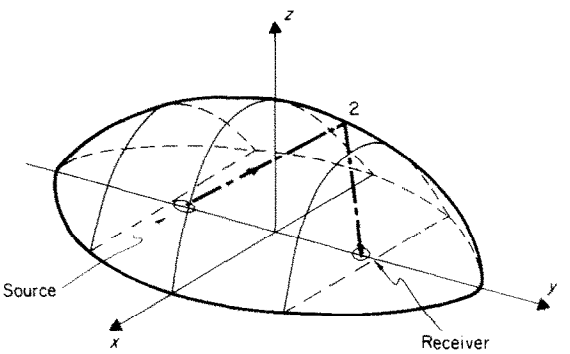

FIG. 1. Pictorial view of integrating hemi-ellipsoid.

The main portion of Fig. 2 is a plan view of the base plane of the ellipsoid. The semi-major and semi-minor radii are a and b respectively, and the focal distances f are given by

$$f/b = \sqrt{[(a/b)^2 - 1]}. \tag{1}$$

The equation of the ellipsoid itself is

$$(x/b)^2 + (y/a)^2 + (z/b)^2 = 1 \tag{2}$$

where it may be noted that the cross sections y = constant are circles.

The radiation source, which is centered at one focus of the base ellipse, has a radius r_s. A photon bundle may leave the source at any

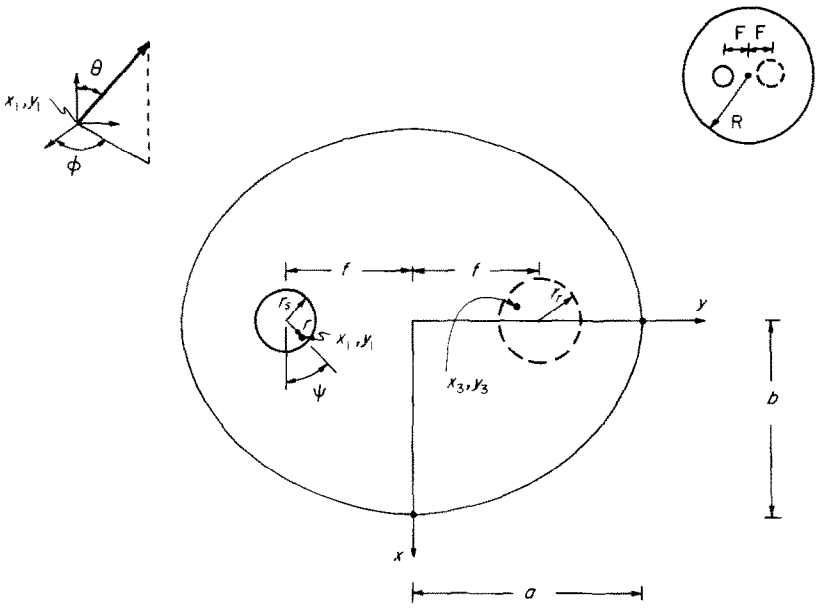

FIG. 2. Co-ordinates and geometrical nomenclature.

point x_1, y_1, the coordinates of which are determined by the laws of probability in conjunction with given information on the surface distribution of the source energy flux. The direction of a departing photon bundle is specified by the angles θ and ϕ that are illustrated by the inset at the upper left of Fig. 2. The departure angles are also determined probabilistically in accordance with radiation property data.

Upon departing from the source point x_1, y_1, the photon bundle travels along a straight line path until it encounters the reflecting surface of the collector. It is postulated that the reflectance of the collector surface is unity* and that the reflection is purely specular. The reflecting surface of the collector redirects the photon bundle towards the base plane, where it impinges at a point x_3, y_3.

The receiver is centered about the second focus of the base ellipse and has a radius r_r. For each given source radius r_s, the collection efficiency corresponding to a succession of receiver radii will be investigated. Correspondingly, the circle depicting the receiver is shown as a dotted line in the figure. The impingement point x_3, y_3 may lie either inside of r_r (as shown in the figure) or outside of r_r.

Governing equations. Attention is first turned to the specifics of determining the departure point x_1, y_1 and the departure angles θ, ϕ. To begin, it is necessary to relate the just-mentioned coordinates and angles to random numbers $R(0 \leq R \leq 1)$ that are provided by a digital computer. An incisive discussion of the basis for such relationships is given by Howell [8]. Generally, it is possible to write

$$r/r_s = \Phi_1(R_1), \quad \psi = \Phi_2(R_2), \quad \theta = \Phi_3(R_3), \quad \phi = \Phi_4(R_4). \tag{3}$$

Explicit forms for $\Phi_1, \ldots, \Phi_4$ will be given later

* If the reflectance is less than unity, then the efficiencies obtained here are to be multiplied by the actual value of the reflectance.

corresponding to specified radiation properties of the source surface and to specified distributions of the leaving radiant flux. For the present, the analytical development will proceed assuming that the Φ functions are known.

In accordance with equation (3), the polar coordinates $r/r_s, \psi$ of the point of departure are calculable as soon as random numbers R_1 and R_2 are drawn. With these, the departure coordinates x_1, y_1 can be written as

$$x_1 = r\cos\psi, \quad y_1 = -f + r\sin\psi. \tag{4}$$

If dimensionless variables are introduced as

$$\hat{x} = x/b, \quad \hat{y} = y/b, \quad \hat{z} = z/b \tag{5}$$

then the foregoing becomes

$$\hat{x}_1 = (r/r_s)(r_s/f)(f/b)\cos\psi,$$
$$\hat{y}_1 = (f/b)[-1 + (r/r_s)(r_s/f)\sin\psi] \tag{6}$$

where f/b is expressed by equation (1).

The selection of random numbers R_3 and R_4 gives the angles θ and ϕ (inset, upper left of Fig. 2) which, in turn, specify the direction of departure of the photon bundle leaving x_1, y_1. To find the intersection of the photon bundle with the curved ellipsoidal surface, an equation is written for the straight line representing the path of the bundle. Simultaneous solution of this equation with that for the ellipsoidal surface [i.e. equation (2)] yields the coordinates of the intersection point 2 shown in Fig. 1.

$$\hat{x}_2 = \hat{x}_1 + \hat{z}_2\cos\phi\tan\theta,$$
$$\hat{y}_2 = \hat{y}_1 + \hat{z}_2\sin\phi\tan\theta \tag{7a}$$
$$\hat{z}_2 = [-B + \sqrt{(B^2 - AC)}]/A \tag{7b}$$

in which

$$A = 1 + [\cos^2\phi + (b/a)^2\sin^2\phi]\tan^2\theta$$
$$B = [\hat{x}_1\cos\phi + (b/a)^2\sin\phi]\tan\theta,$$
$$C = \hat{x}_1^2 + (b/a)\hat{y}_1^2 - 1.$$

It now remains to derive the coordinates of the point 3 where the photon bundle impinges on the base plane after being specularly reflected by the collector at point 2. The normal to the collector surface at point 2 intersects the base plane at a point $x = 0$, $y = y_2[1 - (b/a)^2]$. Furthermore, this point of intersection lies on a straight line which connects points 1 and 3. This information, together with the equality of the angles of incidence and reflection of the photon bundle at point 2, facilitates the trigonometric and algebraic manipulations which yield the expressions for x_3 and y_3. The end result of the derivation is

$$\hat{x}_3 = -\hat{x}_1\zeta,$$
$$\hat{y}_3 = \hat{y}_2\left(1 - \frac{b^2}{a^2}\right)(1 + \zeta) - \hat{y}_1\zeta \tag{8}$$

where

$$\zeta = \frac{\hat{x}_2^2 + (b/a)^4\hat{y}_2^2 + \hat{z}_2^2}{\hat{x}_2(\hat{x}_2 - 2\hat{x}_1) + 2(b/a)^2\hat{y}_2(\hat{y}_2 - \hat{y}_1) - (b/a)^4\hat{y}_2^2 + \hat{z}_2^2}.$$

With x_3 and y_3 thus determined, it remains only to distinguish whether or not the impingement point 3 lies within the confines of the receiver. For this purpose, it is appropriate to examine the sign of the quantity Δ defined by

$$\Delta = r_r - \sqrt{[x_3^2 + (y_3 - f)^2]}. \tag{9}$$

If $\Delta > 0$, the photon bundle impinges on the receiver, while if $\Delta < 0$, the bundle falls outside of the receiver. The receiver radii considered here are expressed relative to the radius r_s of the radiation source; that is, parametric values are assigned to r_r/r_s.

The computational procedure which utilizes the foregoing formulation will now be briefly described. First, a numerical value is assigned for the semi-axis ratio a/b, thereby fixing the dimensionless focal distance f/b via equation (1). Then, the source size is chosen by assigning a

value for r_s/f. For the fixed values of a/b and r_s/f, a succession of photon bundles is released from the source. For each photon bundle, random numbers R_1, R_2, R_3 and R_4 are drawn which, via equation (3), give r/r_s, ψ, θ and ϕ. Sequential application of equations (6)–(8) yields the coordinates x_3, y_3 of the point of impingement of the photon bundle on the base plane. Then, equation (9) is used to distinguish whether or not the impingement is within the confines of a receiver of radius r_r. The latter information is stored for each photon bundle.

After the preselected number of photon bundles for a given parameter pair a/b, r_s/f has all been utilized, the collection efficiency η may be evaluated from

$$\eta = \frac{\text{photon bundles incident on receiver of radius } r_r}{\text{photon bundles leaving source}}. \tag{10}$$

Clearly, η is a function of the receiver radius r_r and, for the present computations, results were obtained for the range $r_r/r_s = 0$ to $r_r/r_s = 2$–3.

The foregoing development was concerned with the integrating hemi-ellipsoid. The modifications appropriate to the integrating hemisphere will now be discussed. For the hemisphere, the semi radii a and b are equal. Therefore, the b/a ratio appearing in equations (7) and (8) is replaced by unity. Furthermore, it may be noted that a hemisphere has only a single focus, which is located at the center of the base plane [equation (1)]. Since the source and receiver cannot overlap one another, they are typically positioned as illustrated in the inset at the upper right of Fig. 2. As shown therein, the centers of the source and receiver circles are situated in conjugate positions along a diametral line, each center being displaced a distance F from the center of the base plane circle.

In light of the foregoing, the computation of the coordinates x_1, y_1 is modified slightly in that the focal distance f in equation (4) is now replaced by F, while f/b in (6) is replaced by F/R, where R is the radius of the hemisphere. The quantity F/R is arbitrarily assignable within reasonable limits. F also replaces f in equation (9), and R is employed as the reference length in lieu of the semi-minor radius b. Aside from the just-discussed modifications, the analysis for the integrating hemi-ellipsoid serves equally well for the integrating hemisphere.

Probability relations. The relationships (3) connect the random numbers R with the coordinates and angles of departure. The explicit forms of these relations depend on the radiation properties of the source surface and on the spatial distribution of the leaving radiation. Inasmuch as the present investigation is intended as a general study of collector characteristics and is not tied to specific surfaces and test conditions, it is appropriate to select a standard case for the numerical computations. A seemingly natural choice for such a standard case is that in which the leaving radiant flux is uniform at all points of the source surface and is diffusely distributed. For this situation, equation (3) becomes

$$r/r_s = \sqrt{R_1}, \quad \psi = 2\pi R_2, \quad \sin\theta = \sqrt{R_3}, \quad \phi = 2\pi R_4. \tag{11}$$

These relationships will emerge from the more general representations given below and may be found, at least in part, in the literature (e.g. [8]).

It is relevant to indicate the probability relations for other cases in addition to those for the standard case cited above. Consider reflection from a test surface having a bi-directional reflectance ρ_{bd} and, for simplicity, suppose that ρ_{bd} is the same at all points on the surface. The test surface is illuminated through an aperture in the curved surface of the collector, and let $e_i(r, \psi)$ denote the surface distribution of incident radiant flux. For this case, the probability relations are

$$R_1 = \frac{\int_0^{2\pi}\int_0^{(r/r_s)} e_i(r/r_s)\,\mathrm{d}(r/r_s)\,\mathrm{d}\psi}{\int_0^{2\pi}\int_0^{1} e_i(r/r_s)\,\mathrm{d}(r/r_s)\,\mathrm{d}\psi}, \quad R_2 = \frac{\int_0^{\psi}\int_0^{1} e_i(r/r_s)\,\mathrm{d}(r/r_s)\,\mathrm{d}\psi}{\int_0^{2\pi}\int_0^{1} e_i(r/r_s)\,\mathrm{d}(r/r_s)\,\mathrm{d}\psi} \tag{12}$$

$$R_3 = \frac{\int_0^{2\pi}\int_0^{\theta} \rho_{bd}\sin 2\theta\,\mathrm{d}\theta\,\mathrm{d}\phi}{\int_0^{2\pi}\int_0^{\pi/2} \rho_{bd}\sin 2\theta\,\mathrm{d}\theta\,\mathrm{d}\phi}, \quad R_4 = \frac{\int_0^{\phi}\int_0^{\pi/2} \rho_{bd}\sin 2\theta\,\mathrm{d}\theta\,\mathrm{d}\phi}{\int_0^{2\pi}\int_0^{\pi/2} \rho_{bd}\sin 2\theta\,\mathrm{d}\theta\,\mathrm{d}\phi}. \tag{13}$$

For the aforementioned standard case where e_i is independent of r and ψ and where ρ_{bd} is independent of θ and ϕ, it is readily verified that equations (12) and (13) reduce to equation (11).

RESULTS AND DISCUSSION

Collection efficiency results for the integrating hemi-ellipsoid are presented in Fig. 3. The efficiency η appears on the ordinate, while the receiver radius r_r, expressed in ratio with the source radius, is the abscissa variable. The curves are parameterized by the ratio a/b of the semi-major radius to the semi-minor radius.

For each a/b appearing in Fig. 3, distributions of η as a function of r_r/r_s were determined for parametric values of the source size parameter r_s/f ranging from 0·1 to 0·5. From a working plot similar to Fig. 3, it was found that for a given a/b, the η value at any r_r/r_s was only affected by one or two in the second decimal place by the aforementioned variation of r_s/f. This insensitivity of collection efficiency to source size parameter is, in itself, a relevant finding which simplifies the design of hemi-ellipsoidal collectors. Owing to the secondary effect of r_s/f, separate curves for specific values of this parameter are not included in Fig. 3.

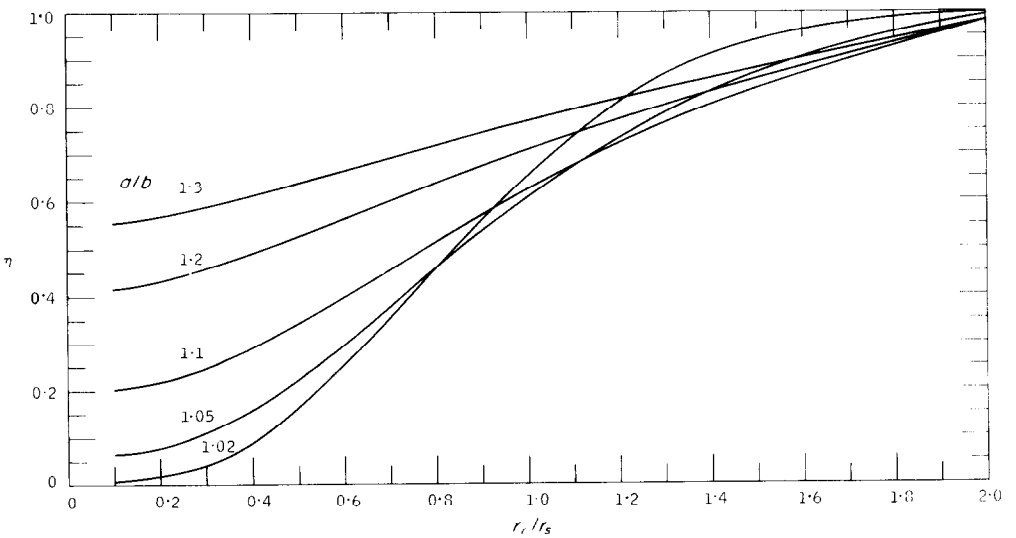

FIG. 3. Collection efficiencies for the integrating hemi-ellipsoid.

An overall inspection of Fig. 3 reveals that nearly one hundred per cent collection is achieved for all of the a/b when the receiver radius is twice that of the source. On the other hand, the collection attained with a receiver having a radius equal to that of the source is inadequate for most purposes. It is also interesting to observe that when the receiver is smaller than the source, there is better collection when the lengths of the major and minor radii are markedly different. For larger receivers, better efficiency is afforded by a collector whose major and minor radii are nearly equal.

In practice, collection efficiencies approaching one hundred per cent are desired for as large a range of r_r/r_s as possible. In light of Fig. 3, this objective is best achieved by ellipsoidal collectors characterized by a/b ratios approaching one. However, in view of the finite size of realistic test surfaces and of the fact that $r_r/r_s > 1$ for good collection, there is a practical lower bound on a/b. In this connection, it may be noted that $a/b = 1{\cdot}042$ for the ellipsoidal collector of [6].

Isolated results for the collection efficiency of an integrating hemi-ellipsoid characterized by $a/b = 1{\cdot}042$ and $r_s/f = 0{\cdot}14$ are reported [6]. A comparison of the results [6] with those interpolated from Fig. 3 indicates that the former are somewhat low. An examination of the causes of the deviations showed that the number of photon bundles employed in the calculations of [6] was not sufficient to give converged results. In addition, there is a small influence of r_s/f which affects the comparison.

Collection efficiencies for integrating hemisphere collectors are shown in Figs. 4 and 5. As before, the efficiency η is plotted as a function of the dimensionless receiver radius. The curves are parameterized by the dimensionless source size r_s/F ranging from 0·1 to 0·5. Figure 4 gives results for the source-receiver position parameter $F/R = 0{\cdot}1$ and 0·15, while Fig. 5 is for $F/R = 0{\cdot}2$ and 0·25.

A general evaluation of these results indicates that for receivers of moderate size ($r_r/r_s \leq 2$), the best efficiencies are attained when the source and receiver are only slightly displaced from the center of the base plane circle (that is, small F/R). Thus, from Fig. 4, it is seen that the collection achieved when $F/R = 0{\cdot}1$ and $r_s/F = 0{\cdot}3$ or 0·5 is comparable to that attained with an ellipsoidal collector. As the displacement of the source and receiver from the center of the base increases (increasing F/R), the collection becomes less efficient, and larger receivers are needed in order to achieve η values of practical interest. In general, in the range of larger efficiencies, better collection is achieved with relatively larger sources (i.e. larger r_s/F).

The results presented in Figs. 3–5 were obtained from computer runs each of which involved 10000 photon bundles. To assess the accuracy of the results, a substantial number of runs were made with 25000 bundles. In all cases, the deviations between the two sets of results were hardly discernible on the scale of the figures. All computations were performed on a CDC 6600 digital computer.

CONCLUDING REMARKS

On the basis of the results, it appears that in the case of the integrating hemi-ellipsoid, the attainment of good collection efficiency requires that the receiver radius be at least twice the source radius. The collection efficiency of the integrating hemisphere is comparable to that of the hemi-ellipsoid when the source and receiver are only slightly displaced from the center of the base plane circle. Otherwise, the hemisphere is a relatively less efficient collector.

The present application of the Monte Carlo method to the evaluation of radiation instrumentation is a further demonstration of the broad utility of this approach. As was implied earlier, a wide range of spatial and directional distributions of the leaving radiation can be treated. Furthermore, non-circular sources and receivers can also be accommodated. Indeed, the only special consideration that need be given to the geometrical shape of the source is to employ appropriate representations for

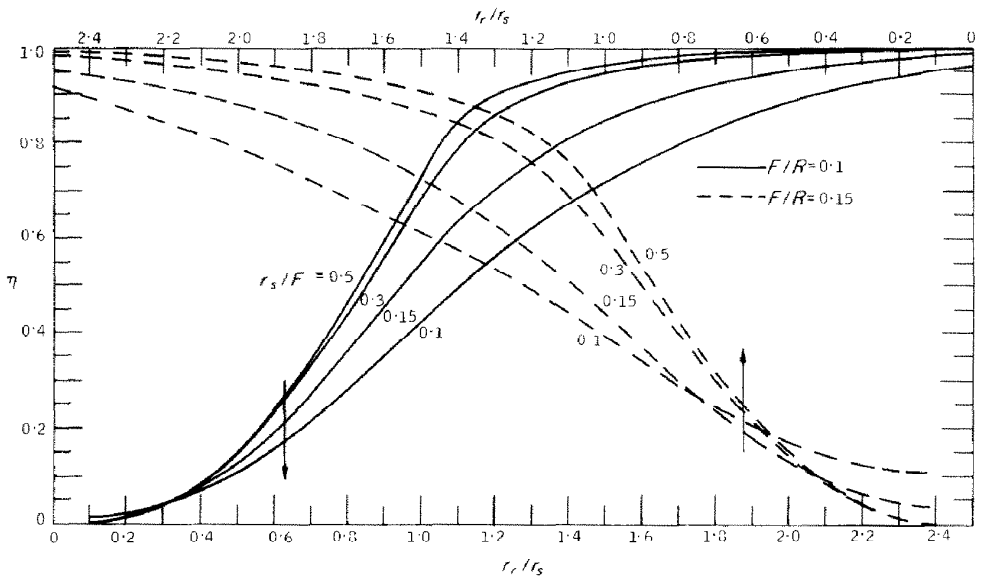

FIG. 4. Collection efficiencies for the integrating hemisphere, $F/R = 0{\cdot}1$ and $0{\cdot}15$.

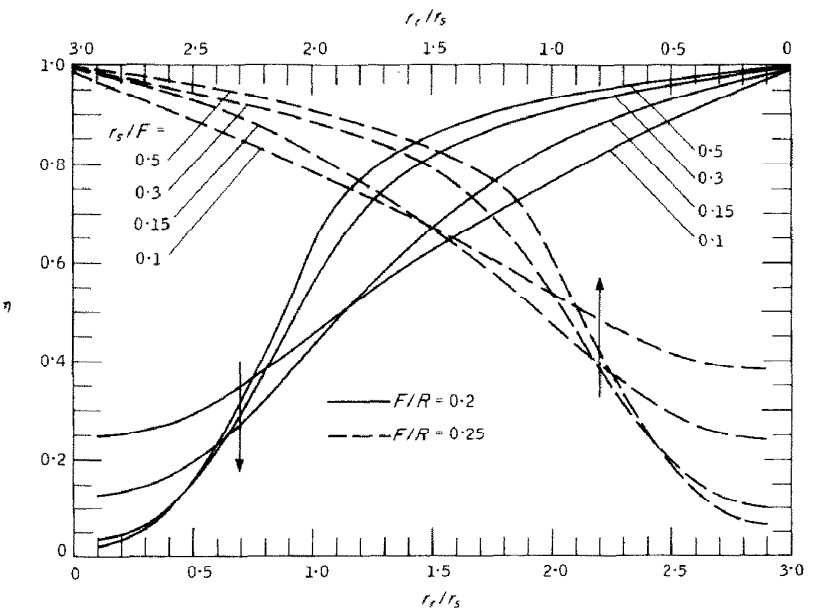

FIG. 5. Collection efficiencies for the integrating hemisphere, $F/R = 0{\cdot}2$ and $0{\cdot}25$.

the coordinates x_1, y_1 of the departure point and, in some cases, it might be advantageous to work with rectangular coordinates rather than with the polar coordinates r, ψ of equation (3). For a non-circular receiver, equation (9) is replaced by an appropriate means of discriminating whether or not the incident photon bundle falls on or outside of the receiver.

REFERENCES

1. T. J. Love, *Radiative Heat Transfer*, pp. 188–190. Merrill, Columbus, Ohio (1968).
2. R. V. Dunkle, Spectral reflectance measurements, *Surface Effects on Spacecraft Materials*, edited by F. J. Clauss, pp. 117–137. John Wiley, New York (1960).
3. T. F. Irvine, Jr., Thermal radiation properties of solids, *Modern Developments in Heat Transfer*, edited by W. E. Ibele, pp. 213–224. Academic Press, New York (1963).
4. J. E. Janssen and R. H. Torberg, Measurement of spectral reflectance using an integrating hemisphere, *Measurement of Thermal Radiation Properties of Solids*, edited by J. C. Richmond, pp. 169–182. NASA SP-31 (1963).
5. R. C. Birkebak, E. M. Sparrow, E. R. G. Eckert and J. W. Ramsey, Effect of surface roughness on the total hemispherical and specular reflectance of metallic surfaces, *J. Heat Transfer* **86C**, 193–199 (1964).
6. R. P. Heinisch, F. J. Bradac and D. B. Perlick, On the fabrication and evaluation of an integrating hemi-ellipsoid, *Appl. Optics* **9**, 483–487 (1970).
7. W. M. Brandenberg, Focusing properties of hemispherical and ellipsoidal mirror reflectometers, *J. Opt. Soc. Am.* **54**, 1235–1237 (1964).
8. J. R. Howell, Application of Monte Carlo to heat transfer problems, *Advances in Heat Transfer*, edited by T. F. Irvine, Jr. and J. P. Hartnett, Vol. 5, pp. 1–54. Academic Press, New York (1968).

CARACTÉRISTIQUES D'EFFICACITÉ DES COLLECTEURS SEMI-ELLIPSOÏDAUX ET HÉMISPHÉRIQUES DE RAYONNEMENT

Résumé—Les rendements de récupération sont déterminés pour des demi-ellipsoïdes et des hémisphères intégrateurs utilisés dans les mesures des propriétés des surfaces rayonnantes. La méthode de Monte-Carlo est employée pour simuler les trajectoires des faisceaux de photons qui quittent une source de rayonnement et sont collectés et focalisés sur (ou adjacent à) un récepteur. La source rayonnante peut être une surface à tester dont la réflectance ou l'émittance sont à déterminer, tandis que le récepteur peut être un détecteur de rayonnement. Des résultats sont obtenus pour une large gamme de dimensions et de positions de sources et de récepteurs. Les résultats montrent que dans le cas du demi-ellipsoïde l'obtention d'un bon rendement de récupération exige que le rayon du récepteur soit au moins deux fois celui de la source. L'hémisphère est en général un collecteur de moindre efficacité que le demi-ellipsoïde. Quand la source et le récepteur sont légèrement déplacés à partir du centre du cercle dans le plan de base de l'hémisphère, alors les deux collecteurs sont d'efficacité comparable.

WIRKUNGSGRAD-CHARAKTERISTIKA VON HALBELLIPSEN UND HALBKUGELN ALS EMPFÄNGER VON TEMPERATURSTRAHLUNG

Zusammenfassung—Es werden die Gesamtwirkungsgrade von Halbellipsoiden und Halbkugeln als Empfänger, wie sie im Zusammenhang mit der Messung der Strahlungseigenschaften von Oberflächen verwendet werden, bestimmt, Die Monte-Carlo-Methode wird angewandt, um die Bahnen von Photonenbündeln zu simulieren, die eine Strahlungsquelle verlassen, dann gesammelt und auf (oder in die Nähe) eines Empfängers fokussiert werden. Die Strahlungsquelle kann eine Testfläche sein, deren Reflexions- oder Emissionsvermögen bestimmt werden soll, während der Empfänger ein Strahlungsdetektor sein mag. Es werden Ergebnisse für einen weiten Bereich der Grössen von Quelle und Empfänger und deren Positionen angegeben. Die Ergebnisse zeigen, dass im Falle des Halbellipsoids der Radius des Empfängers mindestens doppelt so gross sein muss wie der der Quelle, um gute Sammelwirkungsgrade zu erhalten. Im allgemeinen ist die Halbkugel ein weniger wirkungsvoller Kollektor als das Halbellipsoid. Falls die Quelle und der Empfänger nur geringfügig vom Mittelpunkt des Kreises der Basisebene der Halbkugel entfernt werden, sind die beiden Kollektoren ähnlich wirkungsvoll.

ЭФФЕКТИВНОСТЬ ПОЛУЭЛЛИПСОИДНЫХ И ПОЛУСФЕРИЧЕСКИХ ПРИЕМНИКОВ ТЕПЛОВОЙ РАДИАЦИИ

Аннотация—Эффективность поглощения радиации определялась для интегрирующих полуэллипсоидов и полусфер, используемых в связи с определением свойств излучающих

поверхностей. Для моделирования траекторий пучков фотонов, которые выходят из источника излучения, собираются и фокусируются на (или близко к) приемник, применяется метод Монте-Карло. Источником радиации может служить испытуемая поверхность, отражательную или излучательную способность которой нужно определить, тогда как приемник может быть детектором излучения. Получены результаты для большого диапазона размеров и расположений источника и приемника. Результаты показывают, что в случае полуэллипсоида для получения надежных данных по эффективности поглощения радиации необходимо, чтобы радиус приемника был по меньшей мере в два раза больше радиуса источника. Полусфера, в общем, представляет собой менее эффективный коллектор, чем полуэллипсоид. Когда источник и приемник незначительно удалены от центра основного сечения полусферы, тогда оба коллектора сравнительно эффективны.